Chapter 8
Solar Wind Heating by the Turbulent Energy Cascade

The Parker theory (Parker 1958; Parker 1963) predicts an adiabatic expansion of the solar wind from the hot corona without further heating. For such a model, the proton temperature $T(r)$ should decrease with the heliocentric distance r as $T(r) \sim r^{-4/3}$. The radial profile of proton temperature have been obtained from measurements by the Helios spacecraft at 0.3 AU (Marsch et al. 1982; Marsch 1983; Schwenn 1983; Freeman 1988; Goldstein 1996), up to 100 AU or more by Voyager and Pioneer spacecrafts (Gazis 1984; Gazis et al. 1994; Richardson et al. 1995). These measurements show that the temperature decay, at least within fast and Alfvénic wind, is in fact considerably slower than expected. Fits of the radial temperature profile gave an effective decrease $T \sim T_0(r_0/r)^{\xi}$ in the ecliptic plane, with the exponent $\xi \in [0.7; 1]$, much smaller than the adiabatic case. Actually $\xi \simeq 1$ within 1 AU, while ξ flattens to $\xi \simeq 0.7$ beyond 30 AU, where pickup ions probably contribute significantly (Richardson et al. 1995; Zank et al. 1996; Smith et al. 2001a). These observations imply that some heating mechanism must be at work within the wind plasma to supply the energy required to slow down the decay. The nature of the heating process of solar wind is an open problem.

The primary process governing the solar wind heating is probably active locally in the wind. However, since collisions are very rare in the solar wind plasma, the usual viscous coefficients have no meaning, say energy must be transferred to very small scales before it can be efficiently dissipated, perhaps by kinetic processes. As a consequence, the presence of a turbulent energy flux is the crucial first step towards the understanding of solar wind heating (Coleman 1968; Tu and Marsch 1995a) because, as said in Sect. 2.4, the turbulent energy cascade represents nothing but the way for energy to be efficiently dissipated in a high-Reynolds number flow.[1] In other words, before to face the problem of what actually be the physical mechanisms responsible for energy dissipation, if we conjecture that these processes happens at

[1] For a discussion on non-turbulent mechanism of solar wind heating cf. Tu and Marsch (1995a).

R. Bruno, V. Carbone, *Turbulence in the Solar Wind*, Lecture Notes in Physics 928, DOI 10.1007/978-3-319-43440-7_8

small scales, the turbulent energy flux towards small scales must be of the same order of the heating rate.

Using the hypothesis that the energy dissipation rate is equal to the heat addition, one can use the omnidirectional power law spectrum derived by Kolmogorov

$$P(k) = C_K \epsilon_P^{2/3} k^{-5/3}$$

(C_K is the Kolmogorov constant that can be obtained from measurements) to infer the energy dissipation rate (Leamon et al. 1999)

$$\epsilon_P = \left[\frac{5}{3} P(k) C_K^{-1}\right]^{3/2} k^{5/2}, \tag{8.1}$$

where $k = 2\pi f/V$ (f is the frequency in the spacecraft frame and V is the solar wind speed). The same conjecture can be made by using Elsässer variables, thus obtaining a generalized Kolmogorov phenomenology for the power spectra $P^{\pm}(k)$ of the Elsässer variables (Zhou and Matthaeus 1989, 1990; Marsch 1991)

$$\epsilon_P^{\pm} = C_k^{-3/2} P^{\pm}(k) \sqrt{P^{\mp}(k)} k^{5/2}. \tag{8.2}$$

Even if the above expressions are affected by the presence of intermittency, namely extreme fluctuations of the energy transfer rate, and an estimated value for the Kolmogorov constant is required, the estimated energy dissipation rates roughly agree with the heating rates derived from gradients of the thermal proton distribution (MacBride et al. 2010).

A different estimate for the energy dissipation rate in spherical symmetry can be derived from an expression that uses the adiabatic cooling in combination with local heating rate ϵ. In a steady state situation the equation for the radial profile of ions temperature can be written as (Verma et al. 1995)

$$\frac{dT(r)}{dr} + \frac{4}{3}\frac{T(r)}{r} = \frac{m_p \epsilon}{(3/2) V_{\rm SW}(r) k_B}, \tag{8.3}$$

where m_p is the proton mass and $V_{\rm SW}(r)$ is the radial profile of the bulk wind speed in km s^{-1}. (k_B is the Boltzmann constant). Equation (8.3) can be solved using the actual radial profile of temperature thus obtaining an expression for the radial profile of the heating rate needed to heat the wind at the actual value (Vasquez et al. 2007)

$$\epsilon(r) = \frac{3}{2}\left(\frac{4}{3} - \xi\right) \frac{V_{\rm SW}(r) k_B T(r)}{r m_p}. \tag{8.4}$$

This relation is obtained by considering a polytropic index $\gamma = 5/3$ for the adiabatic expansion of the solar wind plasma, the protons being the only particles heated in the process. Such assumptions are only partially correct, since the electrons could play a relevant role in the heat exchange. Heating rates obtained using Eq. (8.4) should

thus be only seen as a first approximation that could be improved with better models of the heating processes. Using the expected solar wind parameters at 1 AU, the expected heating rate ranges from 10^2 J/kg s for cold wind to 10^4 J/kg s in hot wind. Cascade rates estimated from the energy-containing scale of turbulence at 1 AU obtained by evaluating triple correlations of fluctuations and the correlation length scale of turbulence give values in this range (Smith et al. 2001b, 2006; Isenberg 2005; Vasquez et al. 2007)

Rather than estimating the heating rate by typical solar wind fluctuations and the Kolmogorov constant, it is perhaps much more convenient to get a direct estimate of the energy dissipation rate by measurements of the turbulent energy cascade using the Yaglom's law, say from measurements of the third-order mixed moments of fluctuations. In fact, the roughly constant values of $Y_\ell^\pm/\ell$, or alternatively their compressible counterpart $W_\ell^\pm/\ell$ will result in an estimate for the pseudo-energy dissipation rates $\epsilon^\pm$ (at least within a constant of order unity), over a range of scales ℓ, which by definition is unaffected by intermittency. This has been done both in the ecliptic plane (MacBride et al. 2008, 2010) and in polar wind (Marino et al. 2009; Carbone et al. 2009). Preliminary attempts (MacBride et al. 2008) already estimated that the energy dissipation rate ϵ_E was close to the value required for the heating of solar wind. However, refined analysis (MacBride et al. 2010) indicated that at 1 AU, in the ecliptic plane, the solar wind can be sufficiently heated by a turbulent energy cascade. As a different approach, Marino et al. (2009), using data from the Ulysses spacecraft in the polar wind, calculated values of the pseudo-energies from the relation $Y_\ell^\pm/\ell$, and compared these values with the radial profile of the heating rate (8.4) required to maintain the observed temperature against the adiabatic cooling. The Ulysses database provides two different estimates for the temperature, T_1, indicated as $T_{\rm large}$ in literature, and T_2, known as $T_{\rm small}$. In general, T_1 and T_2 are known to give sometimes an overestimate and an underestimate of the true temperature, respectively, so that the analysis was performed using both temperatures (Marino et al. 2008; Marino et al. 2009; Marino et al. 2011). The heating rate was estimated at the same locations where the energy cascade was observed. As shown in Fig. 8.1, results indicate that turbulent transfer rate represents a significant amount of the expected heating, say the MHD turbulent cascade contributes to the in situ heating of the wind from 8 to 50 % (for T_1 and T_2 respectively), up to 100 % in some cases. The authors concluded that, although the turbulent cascade in the polar wind must be considered an important ingredient of the heating, the turbulent cascade alone seems unable to provide all the heating needed to explain the observed slowdown of the temperature decrease, in the framework of the model profile given in Eq. (8.4). The situation is completely different as far as compressibility is taken into account. In fact, when the pseudo-energy transfer rates have been calculated through $W_\ell^\pm/\ell$, the radial profile of energy dissipation rate is well described thus indicating that the turbulent energy cascade provides the amount of energy required to locally heat the solar wind to the observed values.

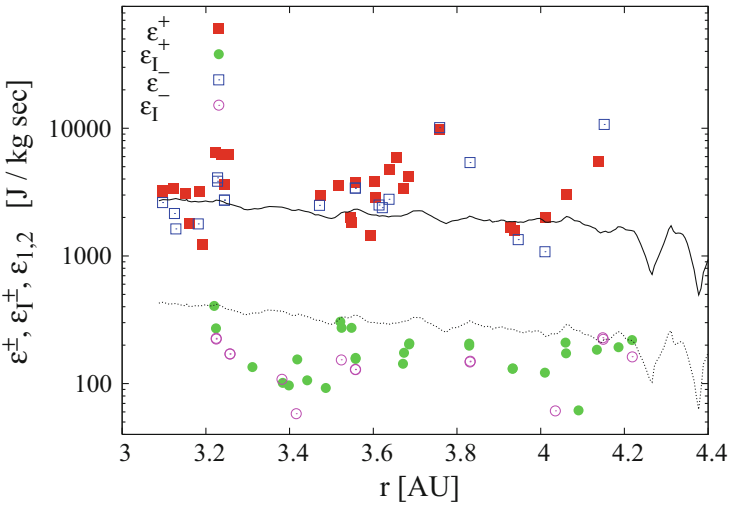

Fig. 8.1 Radial profile of the pseudoenergy transfer rates obtained from the turbulent cascade rate through the Yaglom relation, for both the compressive and the incompressive case. The *solid lines* represent the radial profiles of the heating rate required to obtain the observed temperature profile. Figure adapted from Marino et al. (2011)

8.1 Dissipative/Dispersive Range in the Solar Wind Turbulence

As we saw in Sect. 6.7, the energy cascade in turbulence can be recognized by looking at Yaglom's law. The presence of this law in the solar wind turbulence showed that an energy cascade is at work, thus transferring energy to small scales where it is dissipated by some mechanism. While, as we showed before, the inertial range of turbulence in solar wind can be described more or less in a fluid framework, the small scales dissipative region can be much more (perhaps completely) different. The main motivation for this is the fact that the collision length in the solar wind, as a rough estimate the thermal velocity divided by the collision frequency, results to be of the order of 1 AU. Then the solar wind behaves formally as a collisionless plasma, that is the usual viscous dissipation is negligible. At the same time, in a magnetized plasma there are a number of characteristic scales, then understanding the physics of the generation of the small-scale region of turbulence in solar wind is a challenging topic from the point of view of basic plasma physics. With small-scales we mean scales ranging between the ion-cyclotron frequency $f_{\rm ci} = eB/m_i$ (which in the solar wind at 1 AU is about $f_{\rm ci} \simeq 0.1$ Hz, see Table 1.3), or the ion inertial length $\lambda_i = c/\omega_{pi}$, and the electron-cyclotron frequency $f_{\rm ce} = eB/m_e$. At these scales the usual MHD approximation breaks down in favour of a more complex description of plasma where kinetic processes take place.

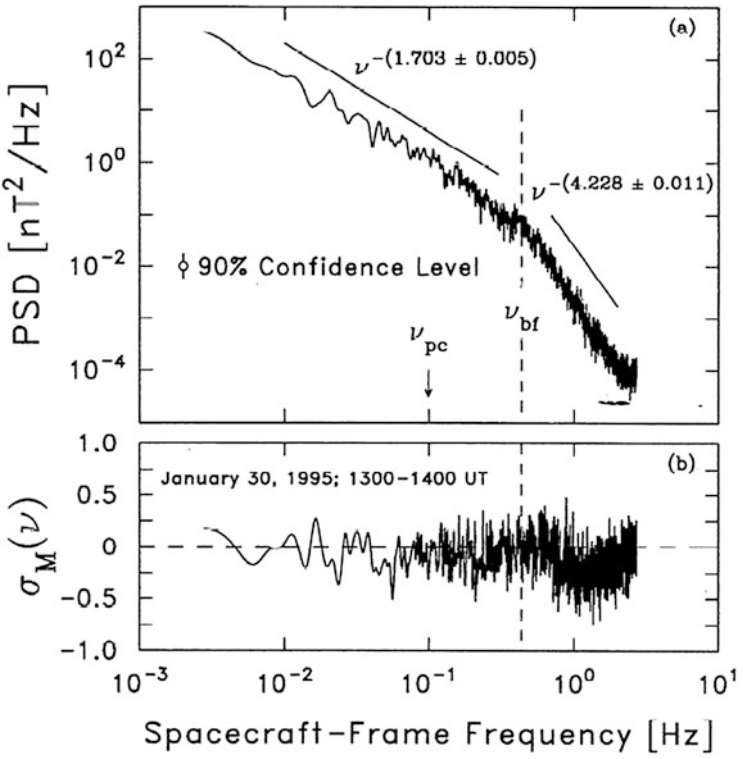

Fig. 8.2 (**a**) Typical interplanetary magnetic field power spectrum obtained from the trace of the spectral matrix. A spectral break at about ~ 0.4 Hz is clearly visible. (**b**) Corresponding magnetic helicity spectrum. Image reproduced by permission from Leamon et al. (1998), copyright by AGU

Some time ago, Leamon et al. (1998) analyzed small-scales magnetic field measurements at 1 AU, by using 33 1-h intervals of the MFI instrument on board Wind spacecraft. Figure 8.2 shows the trace of the power spectral density matrix for hour 13:00 on day 30 of 1995, which is a typical interplanetary magnetic field power spectrum representative of those analysed by Leamon et al. (1998). It is evident that a spectral break exists at about $f_{\rm br} \simeq 0.44$ Hz, slightly above to the ion-cyclotron frequency. Below the ion-cyclotron frequency, the spectrum follows the usual power law $f^{-\alpha}$, where the spectral index is close to the Kolmogorov value $\alpha \simeq 5/3$. At small-scales, namely at frequencies above $f_{\rm br}$, the spectrum steepens significantly, but is still described by a power law with a slope in the range $\alpha \in [2\text{–}4]$ (Leamon et al. 1998; Smith et al. 2006). As a direct analogy to hydrodynamics where the steepening of the inertial range spectrum corresponds to the onset of dissipation, the authors attribute the steepening of the spectrum to the occurrence of a "dissipative" range (Leamon et al. 1998).

In this respect, Smith et al. (2006) performed a wide statistical study on the spectral index in the dissipation range using about 900 intervals of interplanetary

magnetic field recorded by ACE spacecraft at 1 AU. These authors found that while within the inertial range the distribution of the values of the spectral index was quite narrow and peaked between $-5/3$ and $-3/2$ that corresponding to the dissipation range was much broader, roughly varying between -1 and -4 with a broad peak between -2 and -3. These authors were able to correlate this power-law index to the rate of the magnetic energy cascade ϵ. They found steeper dissipation range spectra associated with higher cascade rates. In particular, they found ϵ following $\sim -1.05\epsilon^{0.09}$. These results corroborated previous findings by Leamon et al. (1998) who found that the spectral slope in the dissipation range was directly correlated to the thermal proton temperature, i.e. steeper slopes would imply greater heating rates. Markovskii et al. (2006) found that turbulence spectra often have power-law dissipation ranges with an average spectral index of -3 and suggested that this fact is a consequence of a marginal state of the instability in the dissipation range. However, they concluded that their mechanism, acting together with the Landau damping, would produce an entire range of spectral indices, not just -3, in better agreement with the observations.

Later, Bruno et al. (2014), similarly to previous analyses reported in literature, investigated the behavior of the spectral index within the first frequency decade beyond the spectral break analyzing different solar wind samples along the speed profile of several high velocity streams within the inner heliosphere. They found the same large variability already reported in literature (Leamon et al. 1998; Smith et al. 2006) but were able to highlight a robust tendency for this parameter to indicate steeper spectra within the trailing edge of fast streams and lower values within the subsequent slow wind, following a gradual transition between these two states. These results were successively confirmed also for the parallel and perpendicular spectra (Bruno and Telloni 2015). The value of the spectral index seems to depend firmly on the power associated to the fluctuations within the inertial range, higher the power steeper the slope (see also Smith et al. 2006). In particular, the spectral index tends to approach $-5/3$, typical of the inertial range, within the slow wind while, a simple fit of all the estimates recorded at 1 AU, would suggest a limiting value of roughly -4.2 ± 0.43 within the fast wind. These same authors suggested also that it would be interesting to investigate whether not only the power level of the fluctuations but also their Alfvénic character might play a role in the observed behavior of the spectral index at ion scales in the framework of ion-cyclotron resonance mechanism (see Marsch 2006, and references therein).

Further properties of turbulence in the high-frequency region have been evidenced by looking at solar wind observations by the FGM (flux-gate magnetometer) instrument onboard Cluster satellites (Alexandrova et al. 2008) spanning a $0.02 \div 0.5$ Hz frequency range. The authors found that the same spectral break by Leamon et al. (1998) exists when different datasets (Helios for large-scales and Cluster for small scales) are used. The break (cf. Fig. 1 of Alexandrova et al. 2008) has been found at about $f_{\rm br} \simeq 0.3$ Hz, near the ion cyclotron frequency $f_{\rm ci} \simeq 0.1$ Hz, which roughly corresponds to spatial scales of about 1900 km $\simeq 15\lambda_i$ (being $\lambda_i \simeq 130$ km the ion-skin-depth). However, as shown in Fig. 1 of Alexandrova et al. (2008), the compressible magnetic fluctuations, measured by magnetic field

parallel spectrum $S_\parallel$, are enhanced at small-scales (see Bruno and Telloni 2015; Podesta 2009, and references therein). This means that, after the break compressible fluctuations become much more important than in the low-frequency part. The parameter $\langle S_\parallel \rangle / \langle S \rangle / \simeq 0.03$ in the low-frequency range (S is the total power spectrum density and brackets means averages value over the whole range) while compressible fluctuations are increased to about $\langle S_\parallel \rangle / \langle S \rangle / \simeq 0.26$ in the high-frequency part. The increase of the above ratio were already noted in the paper by Leamon et al. (1998). Moreover, Alexandrova et al. (2008) found that, similarly to the low-frequency region (cf. Sect. 6.2), intermittency is a basic property also in the high-frequency range. In fact, the authors found that PDFs of normalized magnetic field increments strongly depend on the scale (Alexandrova et al. 2008), a typical signature of intermittency in fully developed turbulence (cf. Sect. 6.2). More quantitatively, the behavior of the fourth-order moment of magnetic fluctuations at different frequencies $K(f)$ is shown in Fig. 8.3.

It is evident that this quantity increases with frequency, indicating the presence of intermittency. However the rate at which $K(f)$ increases is pronounced above the ion cyclotron frequency, meaning that intermittency in the high-frequency range is much more effective than in the low-frequency region. Recently, analyzing a different datasets recorded by Cluster spacecraft, it was found that the intermittent character of magnetic fluctuations within the kinetic range persists at least to electron scales (Perri et al. 2012; Wan et al. 2012; Karimabadi et al. 2013) and this was ascribed to the presence of small scale coherent magnetic structures. Further

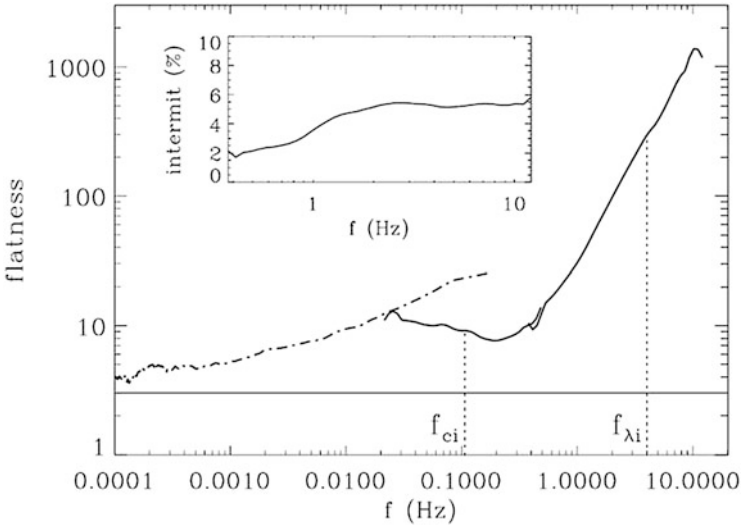

Fig. 8.3 The fourth-order moment $K(f)$ of magnetic fluctuations as a function of frequency f is shown. *Dashed line* refers to data from Helios spacecraft while full line refers to data from Cluster spacecrafts at 1 AU. The *inset* refers to the number of intermittent structures revealed as da function of frequency. Image reproduced by permission from Alexandrova et al. (2008), copyright by AAS

analyses associated elevated plasma temperature and anisotropy events with these structures, suggesting that inhomogeneous dissipation was at work (Servidio et al. 2012).

Different results were obtained by Wu et al. (2013) who, using both flux-gate and search-coil magnetometers on board Cluster, found kinetic scales that are much less intermittent than fluid scales. These authors recorded a remarkable and sudden decrease back to near-Gaussian values of intermittency around scales of about ten times the ion inertial scale (see also results by Telloni et al. 2015; Bruno and Telloni 2015), followed by a modest increase moving toward electron scales, in agreement with Kiyani et al. (2009). These last authors, using high-order statistics of magnetic differences, showed that the scaling exponents of structure functions, evaluated at small scales, are no more anomalous like the low-frequency range, even if Yordanova et al. (2008, 2009) showed that the situation is not so clear.

The above results provide a good example of absence of universality in turbulence, a topic which received renewed attention in the last years (Chapman et al. 2009; Lee et al. 2010; Matthaeus 2009).

8.2 The Origin of the High-Frequency Region

How is the high-frequency region of the spectrum generated? This has become the urgent topic which must be addressed. Ghosh et al. (1996) appeals to change of invariants in controlling the flow of spectral energy transfer in the cascade process, and in this picture no dissipation is required to explain the steepening of the magnetic power spectrum. Furthermore it is believed that the high-frequency region is highly anisotropic, with a significant fraction of turbulent energy cascades mostly in the quasi 2D structures, perpendicular to the background magnetic field. How magnetic energy is dissipated in the anisotropic energy cascade still remains an unsolved and fascinating question.

8.2.1 A Dissipation Range

As we already said, in their analysis of Wind data, Leamon et al. (1998) attribute the presence of the region at frequencies higher than the ion-cyclotron frequency to a kind of dissipative range. Besides analyzing the power spectrum, the authors examined also the normalized reduced magnetic helicity $\sigma_m(f)$ and, they found an excess of negative values at high frequencies. Since this quantity is a measure of the spatial handedness of the magnetic field (Moffatt 1978) and can be related to the polarization in the plasma frame once the propagation direction is known (Smith et al. 1983), the above observations were consistent with the ion-cyclotron damping of Alfvén waves which would leave an excess of kinetic Alfvén waves responsible for the observed value of magnetic helicity. In particular, using a reference system

relative to the mean magnetic field direction $\mathbf{e}_B$ and radial direction $\mathbf{e}_R$ as $(\mathbf{e}_B \times \mathbf{e}_R, \mathbf{e}_B \times (\mathbf{e}_B \times \mathbf{e}_R), \mathbf{e}_B)$, they conclude that transverse fluctuations are less dominant than in the inertial range and the high frequency range is best described by a mixture of 46 % slab waves and of 54 % 2D geometry. Since in the low-frequency range they found 11 and 89 % respectively, the increased slab fraction my be explained by the preferential dissipation of oblique structures. Thermal particles interactions with the 2D slab component may be responsible for the formation of dissipative range, even if the situation seems to be more complicated. In fact they found that also kinetic Alfvén waves propagating at large angles with the background magnetic field might be consistent with the observations and form some portion of the 2D component.

Recently the question of the increased power anisotropy of the high-frequency region has been addressed by Perri et al. (2009) who investigated the scaling behavior of the eigenvalues of the variance matrix of magnetic fluctuations, which provide information on the anisotropy due to different polarizations of fluctuations. These authors investigated data coming from Cluster spacecraft when these satellites orbited in front of the Earth's parallel Bow Shock. Their results showed that magnetic turbulence in the high-frequency region is strongly anisotropic, the minimum variance direction being almost parallel to the background magnetic field at scales larger than the ion cyclotron scale. A very interesting result is the fact that the eigenvalues of the variance matrix have a strong intermittent behavior, with very high localized fluctuations below the ion cyclotron scale. This behavior, never investigated before, generates a cross-scale effect in magnetic turbulence. Indeed, PDFs of eigenvalues evolve with the scale, namely they are almost Gaussian above the ion cyclotron scale and become power laws at scales smaller than the ion cyclotron scale. As a consequence it is not possible to define a characteristic value (as the average value) for the eigenvalues of the variance matrix at small scales. Since the wave-vector spectrum of magnetic turbulence is related to the characteristic eigenvalues of the variance matrix (Carbone et al. 1995), the absence of a characteristic value means that a typical power spectrum at small-scales cannot be properly defined. This is a feature which received little attention, and represents a further indication for the absence of universal characteristics of turbulence at small-scales.

8.2.2 A Dispersive Range

The presence of a frequency range of the magnetic power density spectrum characterized by a clear spectral slope, whose value fluctuates between -2 and -4, (Leamon et al. 1998; Smith et al. 2006; Bruno et al. 2014; Bruno and Telloni 2015), suggests that the high-frequency region above the ion-cyclotron frequency might be interpreted as a kind of different energy cascade due to dispersive effects. Then turbulence in this region can be described through the Hall-MHD models, which is the simplest model apt to investigate dispersive effects in a fluid-like framework. In fact, at variance with the usual MHD, where the effect of ion inertia is taken into

account, the generalized Ohm's law reads

$$\mathbf{E} = -\mathbf{V} \times \mathbf{B} + \frac{m_i}{\rho e}(\nabla \times \mathbf{B}) \times \mathbf{B},$$

where the second term on the r.h.s. of this equation represents the Hall term (m_i being the ion mass). This means that MHD equations are enriched by a new term in the equation describing the magnetic field and derived from the induction equation

$$\frac{\partial \mathbf{B}}{\partial t} = \nabla \times \left[\mathbf{V} \times \mathbf{B} - \frac{m_i}{\rho e}(\nabla \times \mathbf{B}) \times \mathbf{B} + \eta \nabla \times \mathbf{B} \right], \tag{8.5}$$

which is quadratic in the magnetic field. The above equation contains three different physical processes characterized by three different times. By introducing a length scale ℓ and characteristic fluctuations ρ_ℓ, B_ℓ, and u_ℓ, we can define an eddy-turnover time $T_{NL} \sim \ell/u_\ell$, related to the convective process, a Hall time $T_H \sim \rho_\ell \ell^2/B_\ell$ which characterizes typical processes related to the presence of the Hall term, and a dissipative time $T_D \sim \ell^2/\eta$. At large scales the first term on the r.h.s. of Eq. (8.5) describes the Alfvénic turbulent cascade, realized in a time T_{NL}. At very small scales, the dissipative time becomes the smallest timescale, and dissipation takes place.[2] However, one can conjecture that at intermediate scales a cascade is realized in a time which is no more T_{NL} and not yet T_D, rather the cascade is realized in a time T_H. This happens when $T_H \sim T_{NL}$. Since at these scales density fluctuations become important, the mean volume rate of energy transfer can be defined as $\epsilon_V \sim B_\ell^2/T_H \sim B_\ell^3/\ell^2 \rho_\ell$, where T_H is used as a characteristic time for the cascade. Using the usual Richardson's cartoon for the energy cascade which is viewed as a hierarchy of eddies at different scales, and following von Weizsäcker (1951), the ratio of the mass density ρ_ℓ at two successive levels $\ell_v > \ell_{v+1}$ of the hierarchy is related to the corresponding scale size by

$$\frac{\rho_v}{\rho_{v+1}} \sim \left(\frac{\ell_v}{\ell_{nu+1}} \right)^{-3r}, \tag{8.6}$$

where $0 \leq |r| \leq 1$ is a measure of the degree of compression at each level ℓ_v. Using a scaling law for compressive effects $\rho_\ell \sim \ell^{-3r}$ and assuming a constant spectrum energy transfer rate, we have $B_\ell \sim \ell^{(2/3-2r)}$, from which the spectral energy density

$$E(k) \sim k^{-7/3+r}. \tag{8.7}$$

[2] Of course, this is based on classical turbulence. As said before, in the solar wind the dissipative term is unknown, even if it might happens at very small kinetic scales.

The observed range of scaling exponents observed in solar wind $\alpha \in [2\,,4]$ (Smith et al. 2006; Bruno et al. 2014), can then be reproduced by different degree of compression of the solar wind plasma $-5/6 \leq r \leq 1/6$.

8.3 Further Questions About Small-Scale Turbulence

The most "conservative" way to describe the presence of a dissipative/dispersive region in the solar wind turbulence, as we reported before, is for example through the Hall-MHD model. While when dealing with large-scale we can successfully approach the problem of turbulence by saying that some form of dissipation must exist at small-scales, the dissipationless character of solar wind cannot be avoided when we deal with small-scales. The full understanding of the physical mechanisms that allow the dissipation of energy in the absence of collisional viscosity would be a step of crucial importance in the problem of high frequency turbulence in space plasmas. Another fundamental question concerns the dispersive properties of small-scale turbulence beyond the spectral break. This last question has been reformulated by saying: what are the principal constituent modes of small-scale turbulence? This approach explicitly assumes that small-scale fluctuations in solar wind can be described through a weak turbulence framework. In other words, a dispersion relation, namely a precise relationship between the frequency ω and the wave-vector k, is assumed.

As it is well known from basic plasma physics, linear theory for homogeneous, collisionless plasma yields three kind of modes at and below the proton cyclotron frequency Ω_p. At wave-vectors transverse to the background magnetic field and $\Omega_p > \omega_r$ (being ω_r the real part of the frequency of fluctuation), two modes are present, namely a left-hand polarized Alfvén cyclotron mode and a right-hand polarized magnetosonic mode. A third ion-acoustic (slow) mode exists but is damped, except when $T_e \gg T_p$, which is not common in solar wind turbulence. At quasi-perpendicular propagation the Alfvénic branch evolves into Kinetic Alfvén Waves (KAW) (Hollweg 1999), while magnetosonic modes may propagate at $\Omega_p \ll \omega_r$ as whistler modes. As the wave-vector becomes oblique to the background magnetic field both modes develop a nonzero magnetic compressibility where parallel fluctuations become important. There are two distinct scenarios for the subsequent energy cascade of KAW and whistlers (Gary and Smith 2009).

8.3.1 Whistler Modes Scenario

This scenario involves a two-mode cascade process, both Alfvénic and magnetosonic modes which are only weakly damped as the plasma $\beta \leq 1$, transfer energy to quasi-perpendicular propagating wave-vectors. The KAW are damped by Landau damping which is proportional to $k_\perp^2$, so that they cannot contribute to the formation

of dispersive region (unless for fluctuations propagating along the perpendicular direction). Even left-hand polarized Alfvén modes at quasi-parallel propagation suffer for proton cyclotron damping at scales $k_\parallel \sim \omega_p/c$ and do not contribute. Quasi-parallel magnetosonic modes are not damped at the above scale, so that a weak cascade of right-hand polarized fluctuations can generate a dispersive region of whistler modes (Stawicki et al. 2001; Gary and Borovsky 2004, 2008; Goldstein et al. 1994). The cascade of weakly damped whistler modes has been reproduced through electron MHD numerical simulations (Biskamp et al. 1996, 1999; Wareing and Hollerbach 2009; Cho and Lazarian 2004) and Particle-in-Cell (PIC) codes (Gary et al. 2008; Saito et al. 2008).

8.3.2 *Kinetic Alfvén Waves and Ion-Cyclotron Waves Scenario*

In the KAWs scenario (Howes 2008; Schekochihin et al. 2009) long-wavelength Alfvénic turbulence transfer energy to quasi-perpendicular propagation for the primary turbulent cascade up to the thermal proton gyroradius where fluctuations are subject to the proton Landau damping. The remaining fluctuation energy continues the cascade to small-scales as KAWs at quasi-perpendicular propagation and at frequencies $\omega_r > \Omega_p$ (Bale et al. 2005; Sahraoui et al. 2009). Fluctuations are completely damped via electron Landau resonance at wavelength of the order of the electron gyroradius. This scenario has been observed through gyrokinetic numerical simulations (Howes et al. 2008b), where the spectral breakpoint $k_\perp \sim \Omega_p/v_{th}$ (being v_{th} the proton thermal speed) has been observed. In addition, Salem et al. (2012), using Cluster observations in the solar wind, showed that the properties of the small-scale fluctuations are inconsistent with the whistler wave model, but strongly agree with the prediction of a spectrum of KAWs with nearly perpendicular wavevectors.

Several other authors studied the nature of the fluctuations at proton scales near the frequency break f_b (He et al. 2011, 2012b,a; Podesta and Gary 2011; Telloni et al. 2015) adopting new data analysis techniques (Horbury et al. 2008; Bruno et al. 2008). These techniques allowed to infer the polarization of the magnetic fluctuations in a plane perpendicular to the sampling direction and for different sampling directions with respect to the local mean magnetic field orientation, for each scale of interest. These analyses showed the simultaneous signature of polarized fluctuations identified as right-handed KAWs propagating at large angles with the local mean magnetic field and left-handed Alfvén ion-cyclotron waves outward propagating at small angles from the local field. However, Podesta and Gary (2011) remarked that also inward-propagating whistler waves, in the case of a field-aligned drift instability, would give the same left-handed signature like outward-propagating Alfvén ion-cyclotron waves. The presence of KAWs had been already suggested by previous data analyses (Goldstein et al. 1994; Leamon et al. 1998; Hamilton et al. 2008) which, on the other hand, were not able to unravel the simultaneous presence also of left-handed polarized Alfvén ion-cyclotron waves. Figure 8.4 from Telloni et al. (2015) shows the distribution of the normalized

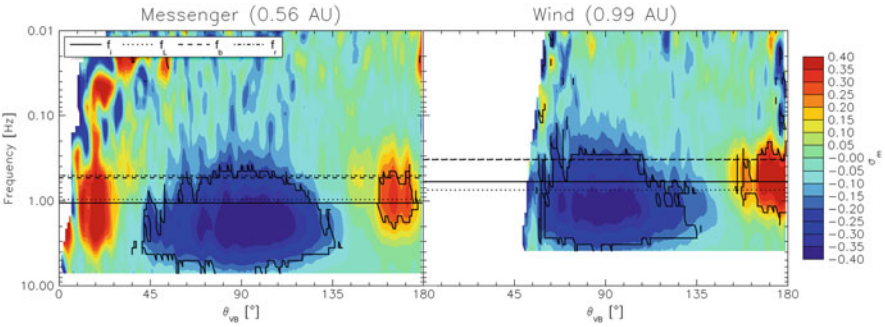

Fig. 8.4 Normalized magnetic helicity, scale by scale, vs the pitch angle θ_{VB} between the local mean magnetic field and the flow direction. Data were collected during a radial alignment between MESSENGER and WIND spacecraft, at 0.56 AU (*left*) and 0.99 AU (*right*), respectively. The *black contour lines* represent the 99 % confidence levels. Characteristic frequencies corresponding to proton inertial length f_i, proton Larmor radius f_L, the observed spectral break f_b and, the resonance condition for parallel propagating Alfvén waves f_r are represented by the *horizontal solid*, *dotted*, *dashed* and *dot-dashed lines*, respectively. Figure adopted from Telloni et al. (2015)

magnetic helicity with respect to the local field pitch angle at MESSENGER (left panel) and WIND (right panel) distances, 0.56 and 0.99 AU, respectively. The frequencies corresponding to the proton inertial length f_i, to the proton Larmor radius f_L, to the observed spectral break f_b, and to the resonance condition for parallel propagating Alfvén waves f_r (Leamon et al. 1998; Bruno and Trenchi 2014), are shown as horizontal solid, dotted, dashed and dot-dashed lines, respectively.

Two populations with opposite polarization can be identified at frequencies right beyond the location of the spectral break. Right-handed polarized KAWs are found for sampling directions highly oblique with respect to the local magnetic field, while left-handed polarized Alfvén ion-cyclotron fluctuations are observed for quasi anti-parallel directions. The same authors found that KAWs dominate the overall energy content of magnetic fluctuations in this frequency range and are largely more compressive than Alfvén ion-cyclotron waves. The compressive character of the KAWs is expected since they generate magnetic fluctuations $\delta B_{\parallel}$ parallel to the local field, particularly for low plasma beta, $\beta \lesssim 1$ (TenBarge and Howes 2012).

Finally, it is interesting to remark that during the wind expansion from Messenger's to WIND's location, the spectral break moved to a lower frequency (Bruno and Trenchi 2014), and both KAWs and Alfvén ion-cyclotron waves shifted accordingly. This observation, per se, is an experimental evidence that relates the location of the frequency break to the presence of these fluctuations (Fig. 8.4).

8.4 Where Does the Fluid-Like Behavior Break Down in Solar Wind Turbulence?

Till now spacecraft observations do not allow us to unambiguously distinguish between both previous scenarios. As stated by Gary and Smith (2009) at our present level of understanding of linear theory, the best we can say is that quasi-parallel whistlers, quasi-perpendicular whistlers, and KAW all probably could contribute to dispersion range turbulence in solar wind. Thus, the critical question is not which mode is present (if any exists in a nonlinear, collisionless medium as solar wind), but rather, what are the conditions which favor one mode over the others. On the other hand, starting from observations, we cannot rule out the possibility that strong turbulence rather than "modes" are at work to account for the high-frequency part of the magnetic energy spectrum. One of the most striking observations of small-scale turbulence is the fact that the electric field is strongly enhanced after the spectral break (Bale et al. 2005). This means that turbulence at small scales is essentially electrostatic in nature, even if weak magnetic fluctuations are present. The enhancement of the electrostatic part has been viewed as a strong indication for the presence of KAW, because gyrokinetic simulations show the same phenomenon (Howes et al. 2008b). However, as pointed out by Matthaeus et al. (2008) (see also the Reply by Howes et al. 2008a to the comment by Matthaeus et al. 2008), the enhancement of electrostatic fluctuations can be well reproduced by Hall-MHD turbulence, without the presence of KAW modes. Actually, the enhancement of the electric field turns out to be a statistical property of the inviscid Hall MHD (Servidio et al. 2008), that is in the absence of viscous and dissipative terms the statistical equilibrium ensemble of Hall-MHD equations in the wave-vectors space is built up with an enhancement of the electric field at large wave-vectors. This represents a thermodynamic equilibrium property of equations, and has little to do with a non-equilibrium turbulent cascade.[3] This would mean that the enhancement of the electrostatic part of fluctuations cannot be seen as a proof firmly establishing that KAW are at work in the dispersive region.

One of the most peculiar possibility from the Cluster spacecraft was the possibility to separate the time domain from the space domain, using the tetrahedral formation of the four spacecrafts which form the Cluster mission (Escoubet et al. 2001). This allows us to obtain a 3D wavevector spectrum and the possibility to identify the actual dispersion relation of solar wind turbulence, if any exists, at small scales. This can be made by using the k-filtering technique which is based on the

[3] It is worthwhile to remark that a turbulent fluid flows is out of equilibrium, say the cascade requires the injection of energy (input) and a dissipation mechanism (output), usually lying on well separated scales, along with a transfer of energy. Without input and output, the nonlinear term of equations works like an energy redistribution mechanism towards an equilibrium in the wave vectors space. This generates an equilibrium energy spectrum which should in general be the same as that obtained when the cascade is at work (cf., e.g., Frisch et al. 1975). However, even if the turbulent spectra could be anticipated by looking at the equilibrium spectra, the physical mechanisms are different. Of course, this should also be the case for the Hall MHD.

strong assumption of plane-wave propagation (Glassmeier et al. 2001). Of course, due to the relatively small distances between spacecrafts, this cannot be applied to large-scale turbulence.

Apart for the spectral break identified by Leamon et al. (1998), a new break has been identified in the solar wind turbulence using high-frequency Cluster data, at about few tens of Hz. In fact, Cluster data in burst mode can reach the characteristic electron inertial scale λ_e and the electron Larmor radius ρ_e. Using the Flux Gate Magnetometer (FGM) (Balogh et al. 2001) and the STAFF-Search Coil (SC) (Cornilleau-Wehrlin et al. 2003) magnetic field data and electric field data from the Electric Field and Wave experiment (EFW) (Gustafsson et al. 2001), Sahraoui et al. (2009) showed that the turbulent spectrum changes shape at wavevectors of about $k\rho_e \sim k\lambda_e \simeq 1$. This result, which perhaps identifies the occurrence of a dissipative range in solar wind turbulence, has been obtained in the upstream solar wind magnetically connected to the bow shock. However, in these studies the plasma β was of the order of $\beta_e \simeq 1$, thus not allowing the separation between both scales. Alexandrova et al. (2009), using three instruments onboard Cluster spacecrafts operating in different frequency ranges, resolved the spectrum up to 300 Hz. They confirmed the presence of the high-frequency spectral break at about $k\rho_e \sim [0.1, 1]$ and, interesting enough, they fitted this part of the spectrum through an exponential decay $\sim \exp[-\sqrt{k\rho_e}]$, thus indicating the onset of dissipation.

The 3D spectral shape reveals poor surprise, that is the energy distribution exhibits anisotropic features characterized by a prominently extended structure perpendicular to the mean magnetic field preferring the ecliptic north direction and also by a moderately extended structure parallel to the mean field (Narita et al. 2010). Results of the 3D energy distribution suggest the dominance of quasi 2D turbulence toward smaller spatial scales, overall symmetry to changing the sign of the wave vector (reflectional symmetry) and absence of spherical and axial symmetry. This last was one of the main hypothesis for the Maltese Cross (Matthaeus et al. 1990), even if bias due to satellite fly through can generate artificial deviations from axisymmetry (Turner et al. 2011).

More interestingly, Sahraoui et al. (2010a) investigated the occurrence of a dispersion relation. They claimed that the energy cascade should be carried by highly oblique KAW with doppler-shifted plasma frequency $\omega_{\text{plas}} \leq 0.1\omega_{ci}$ down to $k_\perp \rho_i \sim 2$. Each wavevector spectrum in the direction perpendicular to an "average" magnetic field $\mathbf{B}_0$ shows two scaling ranges separated by a breakpoint in the interval $[0.1, 1]k_\perp \rho_i$, say a Kolmogorov scaling followed by a steeper scaling. The authors conjectured that the turbulence undergoes a transition-range, where part of energy is dissipated into proton heating via Landau damping, and the remaining energy cascades down to electron scales where Electron Landau damping may dominate. The dispersion relation, compared with linear solutions of the Maxwell–Vlasov equations (Fig. 8.5), seems to identify KAW as responsible for the cascade at small scales. However, the conjecture by Sahraoui et al. (2010a) does not take into account the fact that Landau damping is rapidly saturating under solar wind conditions (Marsch 2006; Valentini et al. 2008).

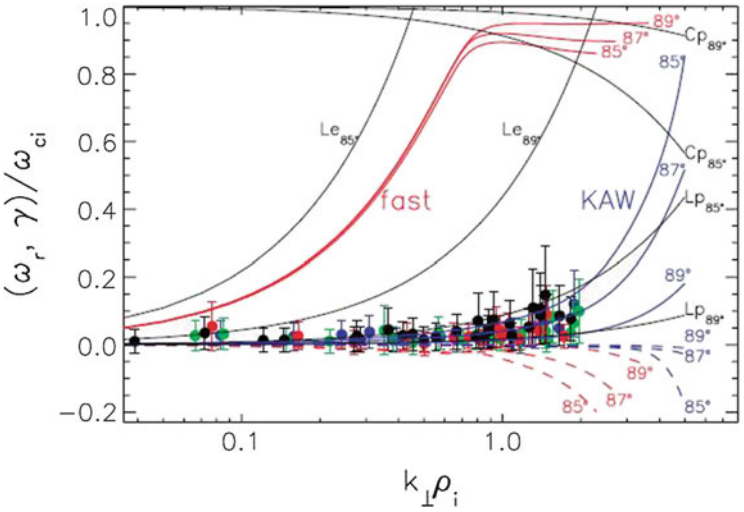

Fig. 8.5 Observed dispersion relations (*dots*), with estimated error bars, compared to linear solutions of the Maxwell–Vlasov equations for three observed angles between the k vector and the local magnetic field direction (damping rates are represented by the *dashed lines*). Proton and electron Landau resonances are represented by the *black curves* $L_{p,e}$. Proton cyclotron resonance are shown by the curves C_p. (the electron cyclotron resonance lies out of the plotted frequency range). Image reproduced by permission from Sahraoui et al. (2010b), copyright by APS

The question of the existence of a dispersion relation was investigated by Narita et al. (2011), who considered three selected time intervals of magnetic field data of CLUSTER FGM in the solar wind. They used a refined version of the *k*-filtering technique, called MSR technique, to obtain high-resolution energy spectra in the wavevector domain. Like the wave telescope, the MSR technique performs fitting of the measured data with a propagating plane wave as a function of frequency and wave vector. The main result is the strong spread in the frequency-wavevector domain, namely none of the three intervals exhibits a clear organization of dispersion relation (see Fig. 8.6). Frequencies and wave vectors appear to be strongly scattered, thus not allowing for the identification of wave-like behavior.

The above discussed papers shed some "darkness" on the scenario of small scales solar wind turbulence as only made by "modes", or at least they indicate that solar wind turbulence, at least at small scales, is far from universality.

Another grey area of investigation is related to the frequency locations of the spectral break separating fluid from kinetic regime.

This break is found at scales of the order of the proton inertial length $\lambda_i = c/\omega_p$ and the proton Larmor radius $\lambda_L = v_{th}/\Omega_p$, where ω_p is the local plasma frequency while Ω_p is the local gyro-frequency, with v_{th} and c the thermal speed and the speed of light, respectively. Several authors tried to match the location of the frequency break with λ_i or λ_L (Perri et al. 2011; Leamon et al. 1998; Bourouaine et al. 2012) with little success. In particular, Markovskii et al. (2008) showed that

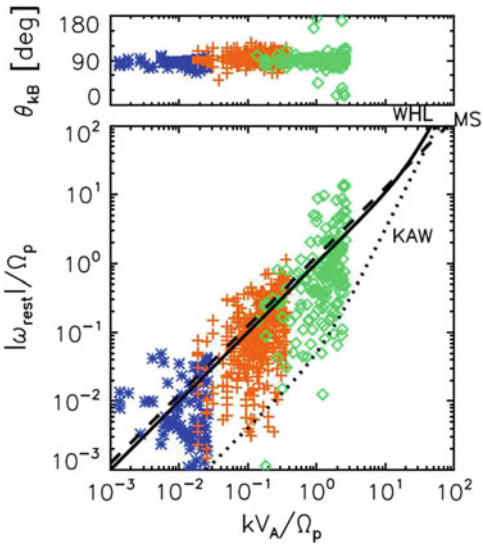

Fig. 8.6 *Top*: Angles between the wave vectors and the mean magnetic field as a function of the wave number. *Bottom*: Frequency-wave number diagram of the identified waves in the plasma rest frame. Magnetosonic (MS), whistler (WHL), and kinetic Alfvén waves (KAW) dispersion relations are represented by *dashed*, *solid*, and *dotted lines*, respectively. Image reproduced by permission from Narita et al. (2011), copyright by AGU

none of the available model could predict a value for the frequency break in good agreement with the observations. Landau damping of obliquely propagating kinetic Alfvén waves (KAW) was proposed by Leamon et al. (1999) and, in this case, the frequency break would correspond to the scale of the Larmor radius λ_L; for Dmitruk et al. (2004) 2-D turbulence dissipation through turbulence reconnection process and generation of current sheets of the order of the ion inertial length λ_i enhances the role of this scale which is the most relevant one also in the framework of incompressible Hall MHD used by Galtier (2006) to explain the break. Only recently, Bruno and Trenchi (2014), using higher time resolution magnetic field data and exploiting selected radial alignments between Messenger, WIND and Ulysses, to restrict the analysis as much as possible to the same fast wind plasma samples, were able to observe a large frequency shift of the high frequency break of about one decade between Messenger location at about 0.42 AU and Ulysses at about 5.3 AU. The same authors found that the resonant condition for outward parallel propagating Alfvén ion-cyclotron waves (ICWs) was the mechanism able to provide the best agreement with the observations, as shown in Fig. 8.7 panel a. Moreover, they showed that this agreement held even taking into account the angle between the background field and the sampling direction, as shown in panel b of the same figure. However, this result was not expected on the basis of anisotropy predictions by any turbulent cascade (Chen et al. 2014) and remains a point which needs to be understood if the ion-cyclotron resonance mechanism for parallel propagating waves is discharged on a theoretical basis.

At this point, having shown that also the high frequency break experiences a shift with distance towards lower frequency, Telloni et al. (2015) proposed a new version of Fig. 3.21 as shown in Fig. 8.8 which unravels the radial behaviour of the whole spectrum between injection and the kinetic scales. Low and high frequency spectral

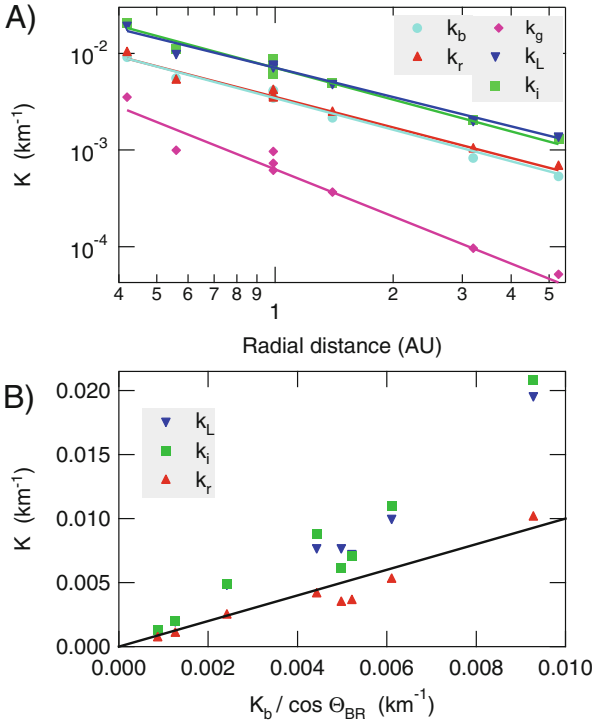

Fig. 8.7 Panel (**a**): radial dependence of wavenumbers associated with the scales corresponding to the observed frequency break κ_b (*cyan circles*), the local proton inertial length κ_i (*blue circles*), the proton Larmor radius κ_L (*green circles*), the wavenumber κ_r corresponding to the resonant condition and the one corresponding to the local cyclotron frequency κ_g (*magenta circles*). The relative best fit curves are shown in the same corresponding colors. Panel (**b**): Wavenumbers associated with the local proton inertial length κ_i (*blue circles*), the proton Larmor radius κ_L (*green circles*) and the wavenumber κ_r (*red circles*) are displayed versus $\kappa_b/\cos(\theta_{BR})$. Figure adopted from Bruno and Trenchi (2014)

breaks move to lower and lower frequencies as the wind expands but their radial dependence is different. The low frequency break has a faster radial evolution $R^{-1.5}$ compared with the high frequency break $R^{-1.1}$. Therefore, the inertial range grows with increasing the heliocentric distance and this confirms previous inferences suggesting that magnetic fluctuations in high speed streams become more and more turbulent with distance (see references in Tu and Marsch 1995b; Bruno and Carbone 2013).

Since the low and high frequency breaks are strictly related to the correlation length λ_C and to the Taylor scale λ_T (see Sect. 3.2.1), respectively, they can be used to determine empirically the effective magnetic Reynolds number R_m^{eff} as (Matthaeus et al. 2005):

$$R_m^{eff} = \left(\frac{\lambda_C}{\lambda_T}\right)^2. \tag{8.8}$$

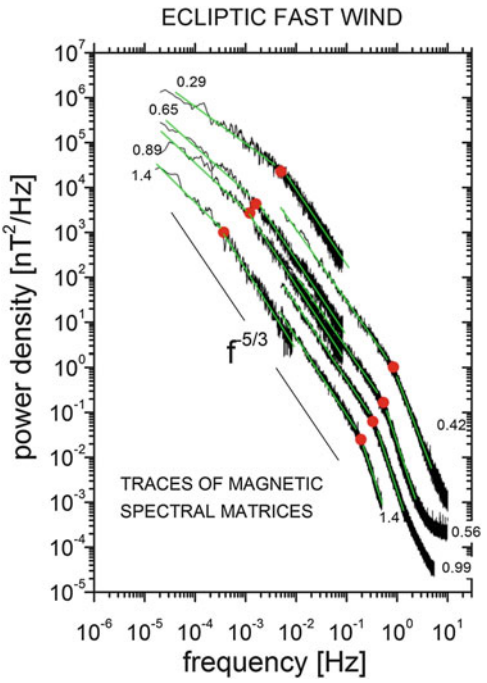

Fig. 8.8 Magnetic field spectral densities for different heliocentric distance as observed by different s/c: MESSENGER (at 0.42 and 0.56 AU), Helios 2 (at 0.29, 0.65 and 0.89 AU), WIND at the Lagrangian point L1 and, ULYSSES at 1.4 AU. Data refer to high speed streams observed in the ecliptic. Low and high frequency breaks are marked by *red dots*. The *solid line* shows, for reference, the Kolmogorov-like spectral slope ($f^{-5/3}$). Figure adopted from Telloni et al. (2015)

In doing so, Telloni et al. (2015) obtained the following values: 3×10^4 at about 0.35 AU, 1.1×10^5 at about 0.65 AU, 1.5×10^5 at about 0.95 AU and, finally, 3.2×10^5 at 1.4 AU. The same authors remarked that the estimate at about 1 AU was in good agreement with the value of 2.3×10^5 provided by Matthaeus et al. (2005) who, using simultaneous measurements of interplanetary magnetic field from the WIND, ACE, and Cluster spacecrafts, were able to build the canonical two-point correlation function.

8.5 What Physical Processes Replace "Dissipation" in a Collisionless Plasma?

As we said before, the understanding of the small-scale termination of the turbulent energy cascade in collisionless plasmas is nowadays one of the outstanding unsolved problem in space plasma physics. In the absence of collisional viscosity and resistivity the dynamics of small-scales is kinetic in nature and must be described by the kinetic theory of plasma. The identification of the physical mechanism that "replaces" dissipation in the collisionless solar wind plasma and establishes a link between the macroscopic and the microscopic scales would open new scenarios in the study of the turbulent heating in space plasmas. This problem is yet in its infancy. Kinetic theory is known since long time from plasma physics, the interested

reader can read the excellent review by Marsch (2006). However, it is restricted mainly to linear theoretical arguments. The fast technological development of supercomputers gives nowadays the possibility of using kinetic Eulerian Vlasov codes that solve the Vlasov–Maxwell equations in multi-dimensional phase space. The only limitation to the "dream" of solving 3D-3V problems (3D in real space and 3D in velocity space) resides in the technological development of fast enough solvers. The use of almost noise-less codes is crucial and allows for the first time the possibility of analyzing kinetic nonlinear effects as the nonlinear evolution of particles distribution function, nonlinear saturation of Landau damping, etc. Of course, faster numerical way to solve the dissipation issue in collisionless plasmas might consist in using intermediate gyrokinetic descriptions (Brizard and Hahm 2007) based on a gyrotropy and strong anisotropy assumptions $k_{\parallel} \ll k_{\perp}$.

As we said before, observations of small-scale turbulence showed the presence of a significant level of electrostatic fluctuations (Gurnett and Anderson 1977; Gurnett and Frank 1978; Gurnett et al. 1979; Bale et al. 2005). Old observations of plasma wave measurements on the Helios 1 and 2 spacecrafts (Gurnett and Anderson 1977; Gurnett and Frank 1978; Gurnett et al. 1979) revealed the occurrence of electric field wave-like turbulence in the solar wind at frequencies between the electron and ion plasma frequencies. Wavelength measurements using the IMP 6 spacecraft provided strong evidence for the presence of electric fluctuations which were identified as ion acoustic waves which are Doppler-shifted upward in frequency by the motion of the solar wind (Gurnett and Frank 1978). Comparison of the Helios results showed that the ion acoustic wave-like turbulence detected in interplanetary space has characteristics essentially identical to those of bursts of electrostatic turbulence generated by protons streaming into the solar wind from the earth's bow shock (Gurnett and Frank 1978; Gurnett et al. 1979). Gurnett and Frank (1978) observed that in a few cases of Helios data, ion acoustic wave intensities are enhanced in direct association with abrupt increases in the anisotropy of the solar wind electron distribution. This relationship strongly suggests that the ion acoustic wave-like structures detected by Helios far from the earth are produced by an electron heat flux instability or by protons streaming into the solar wind from the earth's bow shock. Further evidences (Marsch 2006) revealed the strong association between the electrostatic peak and nonthermal features of the velocity distribution function of particles like temperature anisotropy and generation of accelerated beams.

Araneda et al. (2008) using Vlasov kinetic theory and one-dimensional Particle-in-Cell hybrid simulations provided a novel explanation of the bursts of ion-acoustic activity occurring in the solar wind. These authors studied the effect on the proton velocity distributions in a low-β plasma of compressible fluctuations driven by the parametric instability of Alfvén-cyclotron waves. Simulations showed that field-aligned proton beams are generated during the saturation phase of the wave-particle interaction, with a drift speed which is slightly greater than the Alfvén speed. As a consequence, the main part of the distribution function becomes anisotropic due to phase mixing (Heyvaerts and Priest 1983). This observation is relevant, because the same anisotropy is typically observed in the velocity distributions measured in the fast solar wind (Marsch 2006).

In recent papers, Valentini et al. (2008) and Valentini and Veltri (2009) used hybrid Vlasov–Maxwell model where ions are considered as kinetic particles, while electrons are treated as a fluid. Numerical simulations have been obtained in 1D-3V phase space (1D in the physical space and 3D in the velocity space) where a turbulent cascade is triggered by the nonlinear coupling of circularly left-hand polarized Alfvén waves, in the perpendicular plane and in parallel propagation, at plasma-β of the order of unity. Numerical results show that energy is transferred to short scales in longitudinal electrostatic fluctuations of the acoustic form. The numerical dispersion relation in the $k - \omega$ plane displays the presence of two branches of electrostatic waves. The upper branch, at higher frequencies, consists of ion-acoustic waves while the new lower frequency branch consists of waves propagating with a phase speed of the order of the ion thermal speed. This new branch is characterized by the presence of a plateau around the thermal speed in the ion distribution function, which is a typical signature of the nonlinear saturation of wave-particle interaction process.

Numerical simulations show that energy should be "dissipated" at small-scales through the generation of an ion-beam in the velocity distribution function as a consequence of the trapping process and the nonlinear saturation of Landau damping. This mechanism would produce bursts of electrostatic activity. Whether or not this picture, which seems to be confirmed by recent numerical simulations (Araneda et al. 2008; Valentini et al. 2008; Valentini and Veltri 2009), represents the final fate of the *real* turbulent energy cascade observed at macroscopic scales, requires further investigations. Available plasma measurements in the interplanetary space, even using Cluster spacecrafts, do not allow analysis at typical kinetic scales.

References

O. Alexandrova, V. Carbone, P. Veltri, L. Sorriso-Valvo, Small-scale energy cascade of the solar wind turbulence. Astrophys. J. **674**, 1153–1157 (2008). doi:10.1086/524056

O. Alexandrova, J. Saur, C. Lacombe, A. Mangeney, J. Mitchell, S.J. Schwartz, P. Robert, Universality of solar-wind turbulent spectrum from MHD to electron scales. Phys. Rev. Lett. **103**(16) (2009). doi:10.1103/PhysRevLett.103.165003

J.A. Araneda, E. Marsch, A. F.-Viñas, Proton core heating and beam formation via parametrically unstable Alfvén-cyclotron waves. Phys. Rev. Lett. **100** (2008). doi:10.1103/PhysRevLett.100.125003

S.D. Bale, P.J. Kellogg, F.S. Mozer, T.S. Horbury, H. Reme, Measurement of the electric fluctuation spectrum of magnetohydrodynamic turbulence. Phys. Rev. Lett. **94** (2005). doi:10.1103/PhysRevLett.94.215002

A. Balogh, C.M. Carr, M.H. Acuña, M.W. Dunlop, T.J. Beek, P. Brown, K.-H. Fornaçon, E. Georgescu, K.-H. Glassmeier, J. Harris, G. Musmann, T. Oddy, K. Schwingenschuh, The cluster magnetic field investigation: overview of in-flight performance and initial results. Ann. Geophys. **19**, 1207–1217 (2001). doi:10.5194/angeo-19-1207-2001

D. Biskamp, E. Schwarz, J.F. Drake, Two-dimensional electron magnetohydrodynamic turbulence. Phys. Rev. Lett. **76**, 1264–1267 (1996). doi:10.1103/PhysRevLett.76.1264

D. Biskamp, E. Schwarz, A. Zeiler, A. Celani, J.F. Drake, Electron magnetohydrodynamic turbulence. Phys. Plasmas **6**, 751–758 (1999). doi:10.1063/1.873312

S. Bourouaine, O. Alexandrova, E. Marsch, M. Maksimovic, On spectral breaks in the power spectra of magnetic fluctuations in fast solar wind between 0.3 and 0.9 AU. Astrophys. J. **749**, 102 (2012). doi:10.1088/0004-637X/749/2/102

A.J. Brizard, T.S. Hahm, Foundations of nonlinear gyrokinetic theory. Rev. Mod. Phys. **79**, 421–468 (2007). doi:10.1103/RevModPhys.79.421

R. Bruno, V. Carbone, The solar wind as a turbulence laboratory. Living Rev. Sol. Phys. **10** (2013). doi:10.12942/lrsp-2013-2

R. Bruno, L. Trenchi, Radial dependence of the frequency break between fluid and kinetic scales in the solar wind fluctuations. Astrophys. J. Lett. **787**, 24 (2014). doi:10.1088/2041-8205/787/2/L24

R. Bruno, D. Telloni, Spectral analysis of magnetic fluctuations at proton scales from fast to slow solar wind. Astrophys. J. Lett. **811**, 17 (2015). doi:10.1088/2041-8205/811/2/L17

R. Bruno, E. Pietropaolo, S. Servidio, A. Greco, W.H. Matthaeus, R. D'Amicis, L. Sorriso-Valvo, V. Carbone, A. Balogh, B. Bavassano, Spatial and temporal analysis of magnetic helicity in the solar wind, in *AGU Fall Meeting Abstracts* (2008)

R. Bruno, L. Trenchi, D. Telloni, Spectral slope variation at proton scales from fast to slow solar wind. Astrophys. J. Lett. **793**, 15 (2014). doi:10.1088/2041-8205/793/1/L15

V. Carbone, F. Malara, P. Veltri, A model for the three-dimensional magnetic field correlation spectra of low-frequency solar wind fluctuations during Alfvénic periods. J. Geophys. Res. **100**(9), 1763–1778 (1995). doi:10.1029/94JA02500

V. Carbone, R. Marino, L. Sorriso-Valvo, A. Noullez, R. Bruno, Scaling laws of turbulence and heating of fast solar wind: the role of density fluctuations. Phys. Rev. Lett. **103**(6) (2009). doi:10.1103/PhysRevLett.103.061102

S.C. Chapman, R.M. Nicol, E. Leonardis, K. Kiyani, V. Carbone, Observation of universality in the generalized similarity of evolving solar wind turbulence as seen by Ulysses. Astrophys. J. Lett. **695**, 185–188 (2009). doi:10.1088/0004-637X/695/2/L185

C.H.K. Chen, L. Leung, S. Boldyrev, B.A. Maruca, S.D. Bale, Ion-scale spectral break of solar wind turbulence at high and low beta. Geophys. Res. Lett. **41**, 8081–8088 (2014). doi:10.1002/2014GL062009

J. Cho, A. Lazarian, The anisotropy of electron magnetohydrodynamic turbulence. Astrophys. J. Lett. **615**, 41–44 (2004). doi:10.1086/425215

P.J. Coleman, Turbulence, viscosity, and dissipation in the solar-wind plasma. Astrophys. J. **153**, 371 (1968). doi:10.1086/149674

N. Cornilleau-Wehrlin, G. Chanteur, S. Perraut, L. Rezeau, P. Robert, A. Roux, C. de Villedary, P. Canu, M. Maksimovic, Y. de Conchy, D.H.C. Lacombe, F. Lefeuvre, M. Parrot, J.L. Pinçon, P.M.E. Décréau, C.C. Harvey, P. Louarn, O. Santolik, H.S.C. Alleyne, M. Roth, T. Chust, O. Le Contel, Staff Team, First results obtained by the cluster staff experiment. Ann. Geophys. **21**, 437–456 (2003). doi:10.5194/angeo-21-437-2003

P. Dmitruk, W.H. Matthaeus, N. Seenu, Test particle energization by current sheets and nonuniform fields in magnetohydrodynamic turbulence. Astrophys. J. **617**, 667–679 (2004). doi:10.1086/425301

C.P. Escoubet, M. Fehringer, M. Goldstein, Introduction: the cluster mission. Ann. Geophys. **19**, 1197–1200 (2001). doi:10.5194/angeo-19-1197-2001

J.W. Freeman, Estimates of solar wind heating inside 0.3 AU. Geophys. Res. Lett. **15**, 88–91 (1988). doi:10.1029/GL015i001p00088

U. Frisch, A. Pouquet, J. Leorat, A. Mazure, Possibility of an inverse cascade of magnetic helicity in magnetohydrodynamic turbulence. J. Fluid Mech. **68**, 769–778 (1975). doi:10.1017/S002211207500122X

S. Galtier, Wave turbulence in incompressible hall magnetohydrodynamics. J. Plasma Phys. **72**, 721–769 (2006). doi:10.1017/S0022377806004521

S.P. Gary, J.E. Borovsky, Alfvén-cyclotron fluctuations: linear Vlasov theory. J. Geophys. Res. **109** (2004). doi:10.1029/2004JA010399

S.P. Gary, J.E. Borovsky, Damping of long-wavelength kinetic Alfvén fluctuations: linear theory. J. Geophys. Res. **113** (2008). doi:10.1029/2008JA013565

S.P. Gary, C.W. Smith, Short-wavelength turbulence in the solar wind: Linear theory of whistler and kinetic Alfvén fluctuations. J. Geophys. Res. **114** (2009). doi:10.1029/2009JA014525

S.P. Gary, S. Saito, H. Li, Cascade of whistler turbulence: particle-in-cell simulations. Geophys. Res. Lett. **35** (2008). doi:10.1029/2007GL032327

P.R. Gazis, Observations of plasma bulk parameters and the energy balance of the solar wind between 1 and 10 AU. J. Geophys. Res. **89**, 775–785 (1984). doi:10.1029/JA089iA02p00775

P.R. Gazis, A. Barnes, J.D. Mihalov, A.J. Lazarus, Solar wind velocity and temperature in the outer heliosphere. J. Geophys. Res. **99**, 6561–6573 (1994). doi:10.1029/93JA03144

S. Ghosh, E. Siregar, D.A. Roberts, M.L. Goldstein, Simulation of high-frequency solar wind power spectra using hall magnetohydrodynamics. J. Geophys. Res. **101**, 2493–2504 (1996). doi:10.1029/95JA03201

K.-H. Glassmeier, U. Motschmann, M. Dunlop, A. Balogh, M.H. Acuña, C. Carr, G. Musmann, K.-H. Fornaçon, K. Schweda, J. Vogt, E. Georgescu, S. Buchert, Cluster as a wave telescope - first results from the fluxgate magnetometer. Ann. Geophys. **19**, 1439–1447 (2001). doi:10.5194/angeo-19-1439-2001

M.L. Goldstein, D.A. Roberts, C.A. Fitch, Properties of the fluctuating magnetic helicity in the inertial and dissipation ranges of solar wind turbulence. J. Geophys. Res. **99**, 11519–11538 (1994). doi:10.1029/94JA00789

M.L. Goldstein, Turbulence in the solar wind: kinetic effects, in *Solar Wind Eight*, ed. by D. Winterhalter, J.T. Gosling, S.R. Habbal, W.S. Kurth, M. Neugebauer. AIP Conference Proceedings, vol. 382 (American Institute of Physics, Woodbury, 1996), pp. 239–244. doi:10.1063/1.51391

D.A. Gurnett, R.R. Anderson, Plasma wave electric fields in the solar wind: Initial results from Helios 1. J. Geophys. Res. **82**, 632–650 (1977). doi:10.1029/JA082i004p00632

D.A. Gurnett, L.A. Frank, Ion acoustic waves in the solar wind. J. Geophys. Res. **83**, 58–74 (1978). doi:10.1029/JA083iA01p00058

D.A. Gurnett, E. Marsch, W. Pilipp, R. Schwenn, H. Rosenbauer, Ion acoustic waves and related plasma observations in the solar wind. J. Geophys. Res. **84**, 2029–2038 (1979). doi:10.1029/JA084iA05p02029

G. Gustafsson, M. André, T. Carozzi, A.I. Eriksson, C.-G. Fälthammar, R. Grard, G. Holmgren, J.A. Holtet, N. Ivchenko, T. Karlsson, Y. Khotyaintsev, S. Klimov, H. Laakso, P.-A. Lindqvist, B. Lybekk, G. Marklund, F. Mozer, K. Mursula, A. Pedersen, B. Popielawska, S. Savin, K. Stasiewicz, P. Tanskanen, A. Vaivads, J.-E. Wahlund, First results of electric field and density observations by cluster EFW based on initial months of operation. Ann. Geophys. **19**, 1219–1240 (2001). doi:10.5194/angeo-19-1219-2001

K. Hamilton, C.W. Smith, B.J. Vasquez, R.J. Leamon, Anisotropies and helicities in the solar wind inertial and dissipation ranges at 1 AU. J. Geophys. Res. (Space Phys.) **113**, 01106 (2008). doi:10.1029/2007JA012559

J. He, E. Marsch, C. Tu, S. Yao, H. Tian, Possible evidence of Alfvén-cyclotron waves in the angle distribution of magnetic helicity of solar wind turbulence. Astrophys. J. **731**, 85 (2011). doi:10.1088/0004-637X/731/2/85

J. He, C. Tu, E. Marsch, S. Yao, Do oblique Alfvén/ion-cyclotron or fast-mode/whistler waves dominate the dissipation of solar wind turbulence near the proton inertial length? Astrophys. J. Lett. **745**, 8 (2012a). doi:10.1088/2041-8205/745/1/L8

J. He, C. Tu, E. Marsch, S. Yao, Reproduction of the observed two-component magnetic helicity in solar wind turbulence by a superposition of parallel and oblique Alfvén waves. Astrophys. J. **749**, 86 (2012b). doi:10.1088/0004-637X/749/1/86

J. Heyvaerts, E.R. Priest, Coronal heating by phase-mixed shear Alfven waves. Astron. Astrophys. **117**, 220–234 (1983)

J.V. Hollweg, Kinetic Alfvén wave revisited. J. Geophys. Res. **104**, 14811–14820 (1999). doi:10.1029/1998JA900132

T.S. Horbury, M.A. Forman, S. Oughton, Anisotropic scaling of magnetohydrodynamic turbulence. Phys. Rev. Lett. **807**(17) (2008). doi:10.1103/PhysRevLett.101.175005

G.G. Howes, Inertial range turbulence in kinetic plasmas. Phys. Plasmas **15**(5) (2008). doi:10.1063/1.2889005

G.G. Howes, S.C. Cowley, W. Dorland, G.W. Hammett, E. Quataert, A.A. Schekochihin, T. Tatsuno, Howes et al. reply. Phys. Rev. Lett. **101**(14) (2008a). doi:10.1103/PhysRevLett.101.149502

G.G. Howes, W. Dorland, S.C. Cowley, G.W. Hammett, E. Quataert, A.A. Schekochihin, T. Tatsuno, Kinetic simulations of magnetized turbulence in astrophysical plasmas. Phys. Rev. Lett. **100** (2008b). doi:10.1103/PhysRevLett.100.065004

P.A. Isenberg, Turbulence-driven solar wind heating and energization of pickup protons in the outer heliosphere. Astrophys. J. **623**, 502–510 (2005). doi:10.1086/428609

H. Karimabadi, V. Roytershteyn, M. Wan, W.H. Matthaeus, W. Daughton, P. Wu, M. Shay, B. Loring, J. Borovsky, E. Leonardis, S.C. Chapman, T.K.M. Nakamura, Coherent structures, intermittent turbulence, and dissipation in high-temperature plasmas. Phys. Plasmas **20**(1), 012303 (2013). doi:10.1063/1.4773205

K.H. Kiyani, S.C. Chapman, Y.V. Khotyaintsev, M.W. Dunlop, F. Sahraoui, Global scale-invariant dissipation in collisionless plasma turbulence. Phys. Rev. Lett. **103**(7) (2009). doi:10.1103/PhysRevLett.103.075006

R.J. Leamon, C.W. Smith, N.F. Ness, W.H. Matthaeus, H.K. Wong, Observational constraints on the dynamics of the interplanetary magnetic field dissipation range. J. Geophys. Res. **103**, 4775–4787 (1998). doi:10.1029/97JA03394

R.J. Leamon, C.W. Smith, N.F. Ness, H.K. Wong, Dissipation range dynamics: kinetic Alfvén waves and the importance of β_e. J. Geophys. Res. **104**, 22331–22344 (1999). doi:10.1029/1999JA900158

E. Lee, M.E. Brachet, A. Pouquet, P.D. Mininni, D. Rosenberg, Lack of universality in decaying magnetohydrodynamic turbulence. Phys. Rev. E **81**(1) (2010). doi:10.1103/PhysRevE.81.016318

B.T. MacBride, C.W. Smith, M.A. Forman, The turbulent cascade at 1 AU: energy transfer and the third-order scaling for MHD. Astrophys. J. **679**, 1644–1660 (2008). doi:10.1086/529575

B.T. MacBride, C.W. Smith, B.J. Vasquez, Inertial-range anisotropies in the solar wind from 0.3 to 1 AU: Helios 1 observations. J. Geophys. Res. **115**(A14), 7105 (2010). doi:10.1029/2009JA014939

R. Marino, L. Sorriso-Valvo, V. Carbone, A. Noullez, R. Bruno, B. Bavassano, Heating the solar wind by a magnetohydrodynamic turbulent energy cascade. Astrophys. J. **677**, 71 (2008). doi:10.1086/587957

R. Marino, L. Sorriso-Valvo, V. Carbone, A. Noullez, R. Bruno, B. Bavassano, The energy cascade in solar wind MHD turbulence. Earth Moon Planet. **104**, 115–119 (2009). doi:10.1007/s11038-008-9253-z

R. Marino, L. Sorriso-Valvo, V. Carbone, P. Veltri, A. Noullez, R. Bruno, The magnetohydrodynamic turbulent cascade in the ecliptic solar wind: study of Ulysses data. Planet. Space Sci. **59**, 592–597 (2011). doi:10.1016/j.pss.2010.06.005

S.A. Markovskii, B.J. Vasquez, C.W. Smith, J.V. Hollweg, Dissipation of the perpendicular turbulent cascade in the solar wind. Astrophys. J. **639**, 1177–1185 (2006). doi:10.1086/499398

S.A. Markovskii, B.J. Vasquez, C.W. Smith, Statistical analysis of the high-frequency spectral break of the solar wind turbulence at 1 AU. Astrophys. J. **675**, 1576–1583 (2008). doi:10.1086/527431

E. Marsch, Radial evolution of ion distribution functions, in *Solar Wind Five*, ed. by M. Neugebauer. NASA Conference Publication, vol. 2280 (NASA, Washington, 1983), pp. 355–367

E. Marsch, Turbulence in the solar wind, in *Reviews in Modern Astronomy*, ed. by G. Klare Reviews in Modern Astronomy, vol. 4 (Springer, Berlin, 1991), pp. 145–156

E. Marsch, Kinetic physics of the solar corona and solar wind. Living Rev. Sol. Phys. **3** (2006a). doi:10.12942/lrsp-2006-1

E. Marsch, R. Schwenn, H. Rosenbauer, K. Muehlhaeuser, W. Pilipp, F.M. Neubauer, Solar wind protons: three-dimensional velocity distributions and derived plasma parameters measured between 0.3 and 1 AU. J. Geophys. Res. **87**, 52–72 (1982). doi:10.1029/JA087iA01p00052

W.H. Matthaeus, Prospects for universality in MHD turbulence with cross helicity, anisotropy and shear (invited). Eos Trans. AGU **90**(52), 21–05 (2009)

W.H. Matthaeus, M.L. Goldstein, D.A. Roberts, Evidence for the presence of quasi-two-dimensional nearly incompressible fluctuations in the solar wind. J. Geophys. Res. **95**, 20673–20683 (1990). doi:10.1029/JA095iA12p20673

W.H. Matthaeus, S. Dasso, J.M. Weygand, L.J. Milano, C.W. Smith, M.G. Kivelson, Spatial correlation of solar-wind turbulence from two-point measurements. Phys. Rev. Lett. **95**(23) (2005). doi:10.1103/PhysRevLett.95.231101

W.H. Matthaeus, S. Servidio, P. Dmitruk, Comment on 'kinetic simulations of magnetized turbulence in astrophysical plasmas'. Phys. Rev. Lett. **101**(14) (2008). doi:10.1103/PhysRevLett.101.149501

H.K. Moffatt, *Magnetic Field Generation in Electrically Conducting Fluids*. Cambridge Monographs on Mechanics and Applied Mathematics (Cambridge University Press, Cambridge, 1978)

Y. Narita, K.-H. Glassmeier, F. Sahraoui, M.L. Goldstein, Wave-vector dependence of magnetic-turbulence spectra in the solar wind. Phys. Rev. Lett. **104**(17) (2010). doi:10.1103/PhysRevLett.104.171101

Y. Narita, S.P. Gary, S. Saito, K.-H. Glassmeier, U. Motschmann, Dispersion relation analysis of solar wind turbulence. Geophys. Res. Lett. **38** (2011). doi:10.1029/2010GL046588

E.N. Parker, Dynamics of the interplanetary gas and magnetic fields. Astrophys. J **128**, 664 (1958). doi:10.1086/146579

E.N. Parker, Theory of solar wind, in *Proceedings of the International Conference on Cosmic Rays, Vol. 1: Solar Particles and Sun-Earth Relations* (Tata Institute of Fundamental Research, Bombay, 1963), p. 175

S. Perri, E. Yordanova, V. Carbone, P. Veltri, L. Sorriso-Valvo, R. Bruno, M. André, Magnetic turbulence in space plasmas: scale-dependent effects of anisotropy. J. Geophys. Res. **114**(A13), 2102 (2009). doi:10.1029/2008JA013491

S. Perri, V. Carbone, E. Yordanova, R. Bruno, A. Balogh, Scaling law of the reduced magnetic helicity in fast streams. Planet. Space Sci. **59**, 575–579 (2011). doi:10.1016/j.pss.2010.04.017

S. Perri, M.L. Goldstein, J.C. Dorelli, F. Sahraoui, Detection of small-scale structures in the dissipation regime of solar-wind turbulence. Phys. Rev. Lett. **109**(19), 191101 (2012). doi:10.1103/PhysRevLett.109.191101

J.J. Podesta, Dependence of solar-wind power spectra on the direction of the local mean magnetic field. Astrophys. J. **698**, 986–999 (2009). doi:10.1088/0004-637X/698/2/986

J.J. Podesta, S.P. Gary, Magnetic helicity spectrum of solar wind fluctuations as a function of the angle with respect to the local mean magnetic field. Astrophys. J. **734**, 15 (2011). doi:10.1088/0004-637X/734/1/15

J.D. Richardson, K.I. Paularena, A.J. Lazarus, J.W. Belcher, Radial evolution of the solar wind from IMP 8 to voyager 2. Geophys. Res. Lett. **22**, 325–328 (1995). doi:10.1029/94GL03273

F. Sahraoui, M.L. Goldstein, P. Robert, Y.V. Khotyaintsev, Evidence of a cascade and dissipation of solar-wind turbulence at the electron gyroscale. Phys. Rev. Lett. **102**(23) (2009). doi:10.1103/PhysRevLett.102.231102

F. Sahraoui, M.L. Goldstein, G. Belmont, P. Canu, L. Rezeau, Three dimensional anisotropic k spectra of turbulence at subproton scales in the solar wind. Phys. Rev. Lett. **105**(13), 131101 (2010a). doi:10.1103/PhysRevLett.105.131101

F. Sahraoui, M.L. Goldstein, G. Belmont, P. Canu, L. Rezeau, Three dimensional anisotropic k spectra of turbulence at subproton scales in the solar wind. Phys. Rev. Lett. **105**(13) (2010b). doi:10.1103/PhysRevLett.105.131101

S. Saito, S.P. Gary, H. Li, Y. Narita, Whistler turbulence: particle-in-cell simulations. Phys. Plasmas **15**(10) (2008). doi:10.1063/1.2997339

C.S. Salem, G.G. Howes, D. Sundkvist, S.D. Bale, C.C. Chaston, C.H.K. Chen, F.S. Mozer, Identification of kinetic Alfvén wave turbulence in the solar wind. Astrophys. J. Lett. **745**, 9 (2012). doi:10.1088/2041-8205/745/1/L9

A.A. Schekochihin, S.C. Cowley, W. Dorland, G.W. Hammett, G.G. Howes, E. Quataert, T. Tatsuno, Astrophysical gyrokinetics: kinetic and fluid turbulent cascades in magnetized weakly collisional plasmas. Astrophys. J. Suppl. Ser. **182**, 310–377 (2009). doi:10.1088/0067-0049/182/1/310

R. Schwenn, The 'average' solar wind in the inner heliosphere: structures and slow variations, in *Solar Wind Five*, ed. by M. Neugebauer. NASA Conference Publication, vol. 2280 (NASA, Washington, 1983), pp. 489–507

S. Servidio, W.H. Matthaeus, V. Carbone, Statistical properties of ideal three-dimensional hall magnetohydrodynamics: The spectral structure of the equilibrium ensemble. Phys. Plasmas **15**(4) (2008). doi:10.1063/1.2907789

S. Servidio, F. Valentini, F. Califano, P. Veltri, Local kinetic effects in two-dimensional plasma turbulence. Phys. Rev. Lett. **108**(4), 045001 (2012). doi:10.1103/PhysRevLett.108.045001

C.W. Smith, M.L. Goldstein, W.H. Matthaeus, Turbulence analysis of the Jovian upstream 'wave' phenomenon. J. Geophys. Res. **88**(17), 5581–5593 (1983). doi:10.1029/JA088iA07p05581

C.W. Smith, D.J. Mullan, N.F. Ness, R.M. Skoug, J. Steinberg, Day the solar wind almost disappeared: magnetic field fluctuations, wave refraction and dissipation. J. Geophys. Res. **106**, 18625–18634 (2001a). doi:10.1029/2001JA000022

C.W. Smith, W.H. Matthaeus, G.P. Zank, N.F. Ness, S. Oughton, J.D. Richardson, Heating of the low-latitude solar wind by dissipation of turbulent magnetic fluctuations. J. Geophys. Res. **106**, 8253–8272 (2001b). doi:10.1029/2000JA000366

C.W. Smith, K. Hamilton, B.J. Vasquez, R.J. Leamon, Dependence of the dissipation range spectrum of interplanetary magnetic fluctuations on the rate of energy cascade. Astrophys. J. Lett. **645**, 85–88 (2006). doi:10.1086/506151

O. Stawicki, S.P. Gary, H. Li, Solar wind magnetic fluctuation spectra: dispersion versus damping. J. Geophys. Res. **106**, 8273–8282 (2001). doi:10.1029/2000JA000446

D. Telloni, R. Bruno, L. Trenchi, Radial evolution of spectral characteristics of magnetic field fluctuations at proton scales. Astrophys. J. **805**, 46 (2015). doi:10.1088/0004-637X/805/1/46

J.M. TenBarge, G.G. Howes, Evidence of critical balance in kinetic Alfvén wave turbulence simulations a). Phys. Plasmas **19**(5), 055901 (2012). doi:10.1063/1.3693974

C.-Y. Tu, E. Marsch, MHD structures, waves and turbulence in the solar wind: observations and theories. Space Sci. Rev. **73**(1/2), 1–210 (1995a). doi:10.1007/BF00748891

C.-Y. Tu, E. Marsch, MHD structures, waves and turbulence in the solar wind: observations and theories. Space Sci. Rev. **73**(1/2), 1–210 (1995b). doi:10.1007/BF00748891

A.J. Turner, G. Gogoberidze, S.C. Chapman, B. Hnat, W.-C. Müller, Nonaxisymmetric anisotropy of solar wind turbulence. Phys. Rev. Lett. **107** (2011). doi:10.1103/PhysRevLett.107.095002

F. Valentini, P. Veltri, Electrostatic short-scale termination of solar-wind turbulence. Phys. Rev. Lett. **102**(22) (2009). doi:10.1103/PhysRevLett.102.225001

F. Valentini, P. Veltri, F. Califano, A. Mangeney, Cross-scale effects in solar-wind turbulence. Phys. Rev. Lett. **101**(2) (2008). doi:10.1103/PhysRevLett.101.025006

B.J. Vasquez, C.W. Smith, K. Hamilton, B.T. MacBride, R.J. Leamon, Evaluation of the turbulent energy cascade rates from the upper inertial range in the solar wind at 1 AU. J. Geophys. Res. **112**(A11), 7101 (2007). doi:10.1029/2007JA012305

M.K. Verma, D.A. Roberts, M.L. Goldstein, Turbulent heating and temperature evolution in the solar wind plasma. J. Geophys. Res. **100**, 19839–19850 (1995). doi:10.1029/95JA01216

C.F. von Weizsäcker, The evolution of galaxies and stars. Astrophys. J. **114**, 165 (1951). doi:10.1086/145462

M. Wan, W.H. Matthaeus, H. Karimabadi, V. Roytershteyn, M. Shay, P. Wu, W. Daughton, B. Loring, S.C. Chapman, Intermittent dissipation at kinetic scales in collisionless plasma turbulence. Phys. Rev. Lett. **109**(19), 195001 (2012). doi:10.1103/PhysRevLett.109.195001

C.J. Wareing, R. Hollerbach, Forward and inverse cascades in decaying two-dimensional electron magnetohydrodynamic turbulence. Phys. Plasmas **16**(4) (2009). doi:10.1063/1.3111033

P. Wu, S. Perri, K. Osman, M. Wan, W.H. Matthaeus, M.A. Shay, M.L. Goldstein, H. Karimabadi, S. Chapman, Intermittent heating in solar wind and kinetic simulations. Astrophys. J. **763**, 30 (2013). doi:10.1088/2041-8205/763/2/L30

E. Yordanova, A. Vaivads, M. André, S.C. Buchert, Z. Vörös, Magnetosheath plasma turbulence and its spatiotemporal evolution as observed by the cluster spacecraft. Phys. Rev. Lett. **100**(20) (2008). doi:10.1103/PhysRevLett.100.205003

E. Yordanova, A. Balogh, A. Noullez, R. von Steiger, Turbulence and intermittency in the heliospheric magnetic field in fast and slow solar wind. J. Geophys. Res. **114** (2009). doi:10.1029/2009JA014067

G.P. Zank, W.H. Matthaeus, C.W. Smith, Evolution of turbulent magnetic fluctuation power with heliospheric distance. J. Geophys. Res. **101**, 17093–17108 (1996). doi:10.1029/96JA01275

Y. Zhou, W.H. Matthaeus, Non-WKB evolution of solar wind fluctuations: a turbulence modeling approach. Geophys. Res. Lett. **16**, 755–758 (1989). doi:10.1029/GL016i007p00755

Y. Zhou, W.H. Matthaeus, Transport and turbulence modeling of solar wind fluctuations. J. Geophys. Res. **95**(14), 10291–10311 (1990). doi:10.1029/JA095iA07p10291